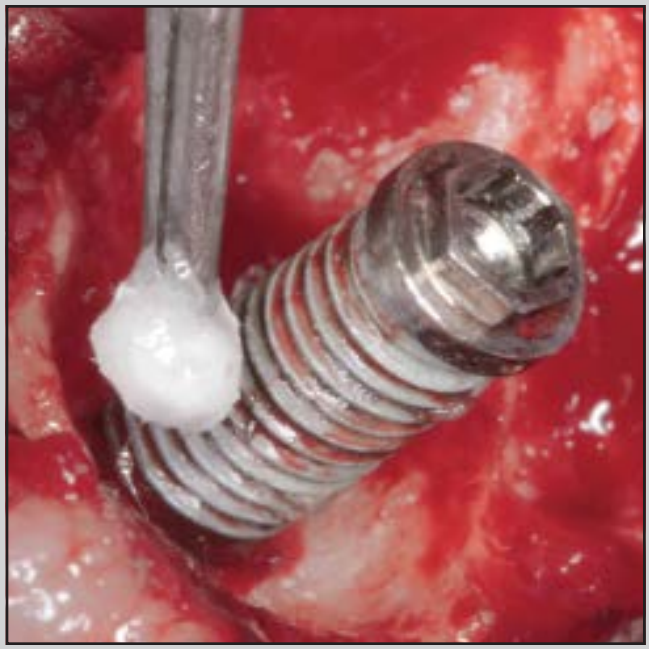

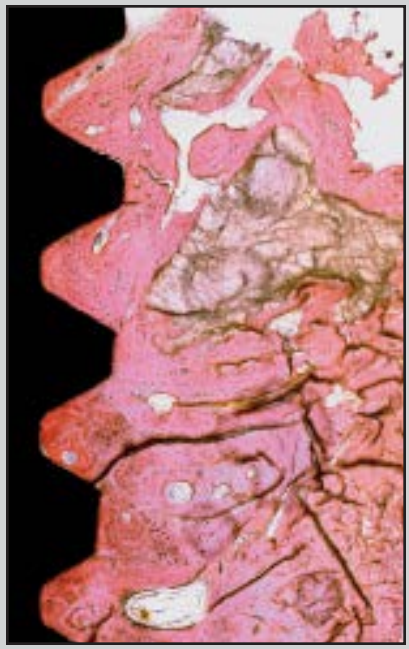

Human Histologic Evidence of Reosseointegration Around an Implant Affected with Peri-implantitis Following Decontamination with Sterile Saline and Antiseptics: A Case History Report

Paul Fletcher, DDS[1]/Daniel Deluiz, DDS, PhD[2]
Eduardo M.B. Tinoco, DDS, PhD[3]
John L. Ricci, PhD[4]/Dennis P. Tarnow, DDS[5]
Justine Monnerat Tinoco, DDS, MS[6]

The treatment of peri-implant disease is one of the most controversial topics in implant dentistry. The multifactorial etiology and the myriad proposed techniques for managing the problem make successful decontamination of an implant surface affected by peri-implantitis one of the more unpredictable challenges dental practitioners have to face. This article presents the first known published case report demonstrating human histologic evidence of reosseointegration using a plastic curette for mechanical debridement and dilute sodium hypochlorite, hydrogen peroxide, and sterile saline for chemical detoxification. Guided bone regeneration in the infrabony component of the peri-implantitis lesion was accomplished using calcium sulfate and bovine bone as grafting materials and a porcine collagen barrier for connective tissue and epithelial exclusion. Int J Periodontics Restorative Dent 2017;37:499–508. doi: 10.11607/prd.3037

[1]Associate Clinical Professor, Division of Periodontics, Columbia University College of Dental Medicine, New York, New York, USA.
[2]Postdoctoral Researcher, Faculty of Dentistry, State University of Rio de Janeiro, Rio de Janeiro, Brazil.
[3]Associate Professor, Faculty of Dentistry, State University of Rio de Janeiro, Rio de Janeiro, Brazil.
[4]Associate Professor, Director of Masters Program, Department of Biomaterials Science, New York University College of Dentistry, New York, New York, USA.
[5]Clinical Professor, Director of Implant Education, Division of Periodontics, Columbia University College of Dental Medicine, New York, New York, USA.
[6]PhD Candidate, Faculty of Dentistry, State University of Rio de Janeiro, Rio de Janeiro, Brazil.

Correspondence to: Dr Paul Fletcher, Specialized Dentistry of New York, 150 E 58th St, Suite 3200, New York, NY 10155, USA. Fax: 212-754-6753. Email: pfletcherdds@gmail.com

The management of peri-implant disease is one of the most controversial topics in implant dentistry today. There are well respected researchers and clinicians who state that peri-implant disease is an occasional occurrence,[1] while equally respected practitioners argue that it is a more significant problem.[2] As the number of implants placed each year and the length of time implants have been in place increase, and as more dentists with varying skills place implants, the number of patients with peri-implant disease is rising.[3,4]

The existing research is confusing. Study methodologies differ. Proposed definitions and thresholds for the presence of mucositis and peri-implantitis are not routinely followed.[4] Different implant surfaces and designs are often combined, and some studies equate implant survival with implant success.[5] There are papers evaluating patients with peri-implant disease while others look at implants with disease.[6] Thus, depending on the study, the prevalence of mucositis after 5 years of function varied from 80% of patients and 50% of implants[7] to 63.4% of patients and 30.7% of implants.[6] The prevalence of peri-implantitis varied from 28% to 56% of patients and 12% to 43% of implants in one paper[7] to 18.8% of patients and 9.6% of implants in another.[6]

Peri-implant disease is multifactorial. Clinician-related factors include improper implant placement, surgical trauma, and faulty prosthetic design. Patient-associated factors include a predisposition to periodontal disease, inadequate oral hygiene and a lack of professional maintenance, absence of attached gingiva, smoking, bone quality, and certain systemic diseases and medications. Implant-related factors include the type of materials used, one-stage versus two-stage construction, thread design, and surface modifications.[1] In addition to the physical contour of the implant restoration and microleakage of bacteria in and out of the implant-abutment junction, the macroanatomy of the implant threads and the microanatomy of the implant surface present a unique challenge. Thorough debridement of the implant is unpredictable by mechanical means alone, as the undercuts of the screw-shaped threads and the adhesion of microbes in the concavities of a roughened implant surface can make access to accretions and their removal extremely difficult.[8]

Chemical adjuncts[9] have consequently been used in conjunction with mechanical debridement to disrupt plaque biofilm, dilute bacterial concentrations to a subinflammatory level, destroy the organic components of bacteria, and remove residual bacterial cell wall endotoxin. The ultimate objectives of treatment are to eliminate inflammation, reduce pocketing, stabilize bone levels, or regenerate bone that has previously been lost.

Numerous mechanical and chemical surface decontamination protocols and techniques have been presented in the literature, including the use of curettes, sonics and ultrasonics, air polishers, lasers, titanium brushes, chlorhexidine, sterile saline, sodium hypochlorite, citric acid, povidone iodine, stannous fluoride, chloramine-T, EDTA, local and systemic antibiotics, hydrogen peroxide, biologics, essential oil mouthwash, triclosan dentifrice, polishing cup and brush, glow discharge, and photodynamic therapy.[10–15] As has been succinctly stated, while there is no reliable evidence that any one of these treatments is the most effective for managing peri-implant disease, this doesn't mean they do not work.[16] If peri-implant disease is an ongoing problem, the worldwide dental community would benefit if a readily available, simple-to-use, low-cost means of detoxifying an implant surface was shown to be effective.

Multiple animal studies have histologically evaluated surface decontamination and bone regeneration around an implant affected by peri-implantitis. Sterile saline (SS) was used as a control in numerous instances and proved to be as effective as the treatment being tested.[17–19] While to date there is no human histology showing the effectiveness of SS for surface decontamination during open flap debridement, a 4-year longitudinal clinical study comparing its efficacy to an Er:YAG laser under the same conditions found no ongoing clinical superiority for either technique.[20]

This case report will present the histologic results of a regenerative protocol for the treatment of inflammatory peri-implantitis.

Materials and Methods

A healthy, nonsmoking, 56-year-old man presented at the dental clinic of the Department of Periodontics of the State University of Rio de Janeiro Brazil in January 2015 with a mandibular screw-retained implant overdenture replacing all teeth from the right first molar to the left first premolar. The restoration had been inserted approximately 5 years prior and was supported by five 3.75 × 13-mm screw-retained implants (Mk III, Nobel Biocare) spaced in the arch between the positions of the canines. The patient was partially edentulous in his maxilla, with all incisors and canines and the left second premolar remaining. While he had an abundance of keratinized gingiva, 7 to 10 mm of pocketing, bleeding on probing, and soft tissue redness and inflammation were evident around all implants. The patient's oral hygiene was poor, as heavy plaque and calculus accumulations were readily visible (Fig 1). The radiographs confirmed the clinical findings showing advanced bone loss around all five implants. For identification purposes, the implant in the mandibular right canine position was labeled implant 1, with the implant to the right of it when looking at the radiographs labeled implant 2, the center implant 3, the fourth implant from the left 4, and the implant in the left canine position 5 (Fig 2). The proposed treatment plan was to remove implants 2 and 3 and augment the extraction sites for future implant placement while simultaneously attempting to regenerate bone around implants 1,

Fig 1 *Preoperative photo of plaque and calculus accumulations and soft tissue inflammation around all implants.*

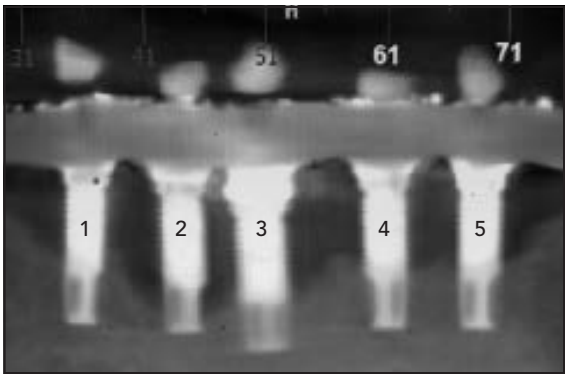

Fig 2 *Preoperative panoramic radiograph. The test implant is marked with the number 3.*

4, and 5. After further evaluation of a cross-sectional radiograph showing the size and shape of the bony defect around implant 3 (Fig 3), the patient was asked if he would allow us to retain implant 3 and graft and treat it similarly to implants 1, 4, and 5 prior to subsequently removing it for histologic evaluation. A study protocol was developed at the State University of Rio de Janeiro and approved by the Ethics Committee of the University Hospital Pedro Ernesto (CE-HUPE) in full accordance with the World Medical Association Declaration of Helsinki. The patient accepted it and gave his oral and written informed consent prior to treatment.

The patient was placed on amoxicillin 250 mg and metronidazole 250 mg tid for 10 days beginning 1 day prior to the surgery. He was anesthetized at the beginning of the procedure using 2% lidocaine with 1:100,000 epinephrine (DFL). The mandibular restoration was removed and a red, inflamed gingiva that bled on probing was visualized around all five implants (Fig 1). All loose supragingival debris was removed prior to initiating further treatment.

A surgical incision was made on the crest of the ridge extending intrasulcularly around the implants. Full-thickness buccal and lingual flaps were reflected. Adequate extension beyond implants 1 and 5 eliminated the need for vertical incisions, and adequate internal release avoided muscle tension on the buccal flap. A large curette (Prichard, Hu-Friedy) was used to mechanically debride the granulomatous tissue from the bony defects around the implants. Implant 2 was removed at this time. To mechanically clean the plaque and calculus present on all the implant surfaces, a plastic curette (Implacare II, Hu-Friedy) was used to carefully go around and into each of the implant threads (Fig 4a). Once the bony defects and the implants were thoroughly debrided mechanically, the entire surgical site was rinsed with copious amounts of SS from an irrigating syringe with the tip of the syringe close to the threads of the implant.

Fig 3 *Cross-sectional computed tomography scan of the test implant.*

Following mechanical debridement, 5 mL of 5% to 6% sodium hypochlorite (NaClO) (standard household bleach) was combined with 125 mL of sterile water, forming a 0.25% solution of NaClO. Small cotton pellets saturated with the solution were used with firm pressure to meticulously clean 360 degrees around the implant collar and between the implant threads (Fig 4b). After burnishing for approximately 1 minute, the solution was rinsed off using SS in an irrigating syringe. A 1.5% hydrogen peroxide (H_2O_2) solution, formed by mixing equal amounts of 3% H_2O_2 and sterile water, was then applied using the same protocol.

Fig 4a *A plastic curette is used in a circular direction around each implant thread to remove or disrupt the plaque and calculus on the implant surface.*

Fig 4b *A cotton pellet is used to meticulously burnish antiseptic on the platform and around and between each implant thread to chemically detoxify the implant surface.*

Fig 4c *The implant platform has been sectioned from the test implant. The size and shape of the infrabony defect can be visualized. A total of 11 implant threads are exposed, 8 within the walls of the infrabony defect.*

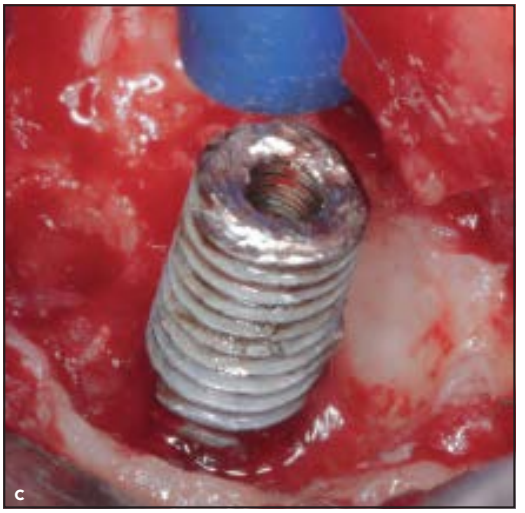

At this point the platform of test implant 3 was sectioned from its body to facilitate submerging the implant during the healing process. The depth of the infrabony defect was quantified by counting the number of exposed threads from the base of the defect to the top of the implant. A total of 11 threads were exposed, 8 of which were within the walls of the infrabony defect. The defect was 6 mm at its widest. The screw access opening of the test implant was thoroughly detoxified with NaClO but was not closed with a cover screw. SS was burnished on the surfaces of all the implants, and the entire surgical site was rinsed again with SS (Fig 4c).

Following mechanical and chemical detoxification, three porcine membranes (Dynamatrix, Keystone Dental) were prepared for GBR on implants 1, 3, 4, and 5. Using a 4-mm tissue punch, a 4-mm-diameter hole was made in the center of two of the membranes so one would precisely fit over implant 1 and the other over test implant 3. The third membrane was centered over implants 4 and 5, and small holes were placed through it using an explorer point into the screw access openings of the implants. These holes were subsequently enlarged with the 4-mm tissue punch so the membrane would accurately fit over both implant heads. The membranes were set aside and the bone-grafting material was prepared.

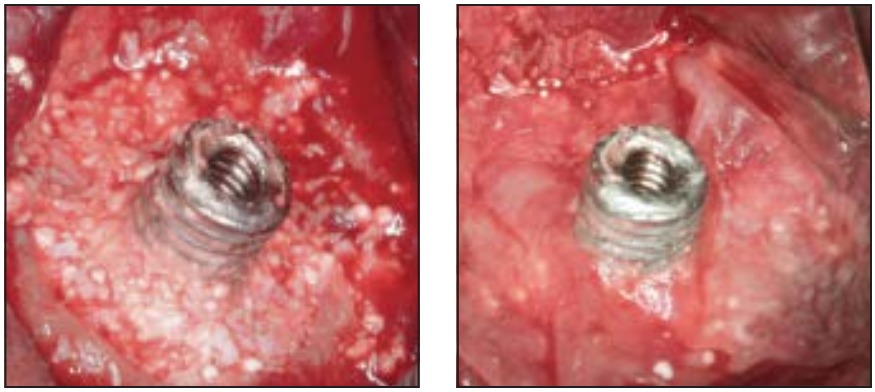

Fig 5a (left) *The infrabony defect has been filled with a 50:50 mix of nanocrystalline $CaSO_4$ and bovine bone.*

Fig 5b (right) *A porcine collagen membrane with a 4-mm-diameter opening in the center has been placed over the test implant to completely cover the graft.*

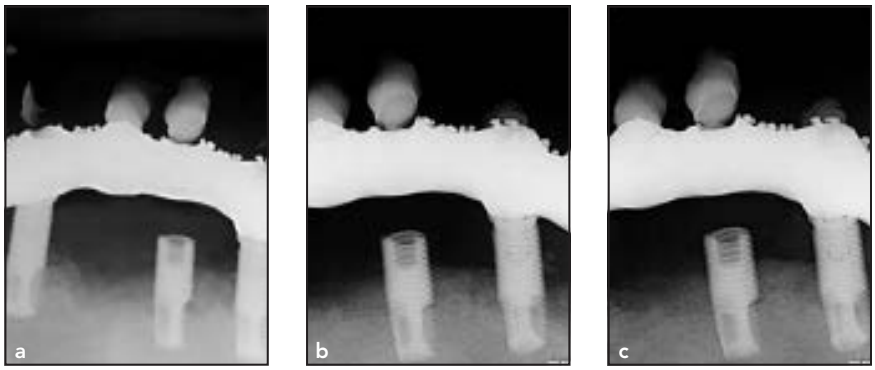

Fig 6 *Postoperative radiographs at* (a) *1 week,* (b) *4 months, and* (c) *6 months showing bone levels around the test implant.*

Nanocrystalline calcium sulfate ($CaSO_4$) (Nanogen, Orthogen) and small-particle bovine bone (BB) (Bio-Oss, Geistlich) were used to graft the infrabony defects. Equal amounts by volume of each were combined and hydrated with the setting liquid provided with the $CaSO_4$. The mix was then incrementally packed with moderate density into the apical aspect of the defects, with an effort made to obtain close graft-to-implant surface approximation 360 degrees around the implant. Successive increments of bone mix were hydrated and layered on top of the first mix and also used to graft the socket where implant 2 had been removed (Fig 5a). Once the defects were filled and the excess graft material removed, the holes in the porcine membranes were carefully placed over the heads of the implants and the membranes were maneuvered apically until they covered the bone grafts and rested on the buccal and lingual plates and the interimplant ridge (Fig 5b).

The buccal and lingual flaps were passively replaced and sutured to cover the entire test implant and the supracrestal threads of the three exposed implants. To stabilize the blood clot, continuous gentle pressure was applied for 1 minute at the point where the buccal and lingual gingiva met the implant collar. The underside of the restoration was recontoured and decontaminated and then replaced. The patient was instructed to continue with the prescribed antibiotics, brush his maxillary teeth normally, and rinse around his lower bridge with salt water rinses and an essential oil mouthwash (Listerine, Johnson & Johnson) twice a day for 30 seconds.

Appointments followed at 1 week, 2 weeks, 1 month, 2 months, and 4 months postoperative. At these visits, the exposed implant surfaces were debrided, periapical radiographs were taken as needed (Fig 6), and the patient's oral hygiene was reinforced and modified as necessary.

Fig 7 *At the time of reentry, a probe could be inserted through a small communication by the head of the test implant.*

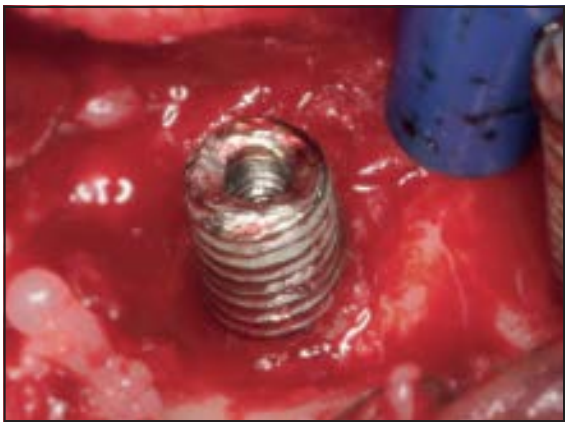

Fig 8 *Bone fill is visible around the test implant on reentry. A total of 8 implant threads are now exposed, 5 within the confines of the infrabony defect.*

A reentry procedure was performed 6 months after the initial surgery. After the patient gave verbal and written informed consent, preoperative radiographs were taken, the framework was removed, and the patient was anesthetized as before. A crestal incision over the test implant was extended laterally, and buccal and lingual mucoperiosteal flaps were reflected. The test implant and a circumferential collar of bone in contact with the apical aspect of the implant was removed using a piezo (PiezoMed SA-320, W&H Dentalwerk) and a trephine with an internal diameter of 7 mm. The site where the implant was removed was grafted with BB and covered with a porcine membrane. The supracrestal threads of the remaining implants were debrided and detoxified, the gingival flaps were approximated and sutured, and the framework was decontaminated and replaced.

The implant/bone core was placed in 10% neutral buffered formalin, fixed for 24 hours, and rinsed and stored in gauze soaked in phosphate-buffered saline. It was subsequently transferred to different alcohol concentrations and then sectioned with a low-speed saw (IsoMet, Buehler) to separate the superosseous portion from the portion that was incorporated in bone. The supracrestal section was examined using an EVO 50 environmental scanning electron microscope (SEM) (Zeiss) at low vacuum, with no carbon or gold coating, and an S3500N SEM (Hitachi) using a backscattered imaging mode and high contrast.

The portion of the implant in bone was embedded in polymethyl methacrylate, sectioned, glued on a Plexiglas slide, ground down, and polished to a thickness of approximately 100 µm. The sample was carbon coated, and SEM images were viewed using a backscattered imaging mode with the Hitachi S3500N in a high-contrast mode. The histologic slides were prepared by wiping off the carbon coating and staining the sample with a combination of Stevenel blue and van Gieson picrofuchsin and imaged with a slide scanner (ScanScopeGL, Aperio).

Results

At reentry, a small soft tissue communication that allowed for the insertion of a periodontal probe was evident over the top of the test implant (Fig 7). Following flap reflection, the coronal bone fill in the infrabony defect around the test implant was quantified by counting the number of exposed threads. Eight threads were exposed, 5 within the walls of the residual infrabony defect (Fig 8).

A low-power SEM of the superosseous implant surface shows the macroanatomy of the implant threads. Flattened areas visible on the edges of the threads were caused by pressure from the beaks of an instrument used to stabilize the specimen during the sectioning process. No organic material is evi-

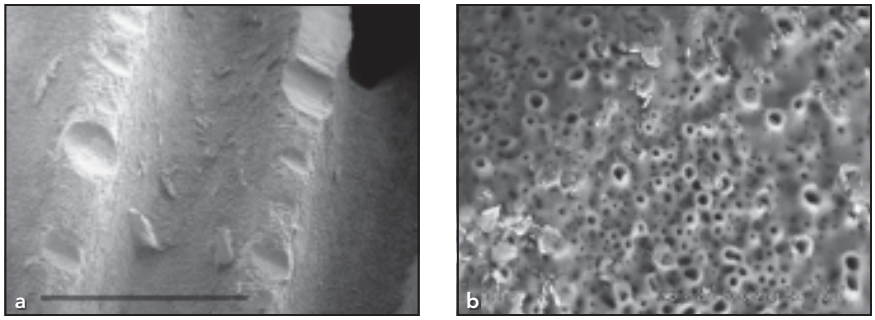

Fig 9a *Low-magnification SEM image showing the macroanatomy of the supracrestal implant threads. While processing debris that has flaked off the implant surface is visible, large accumulations of bacteria and calcified material are absent. Scale bar = 600 µm.*

Fig 9b *Higher-magnification SEM showing the microanatomy of the additive anodized surface. The microporous surface shows no bacteria, but some particles of mineralized material remain in and around the cryptlike openings. Scale bar = 30 µm.*

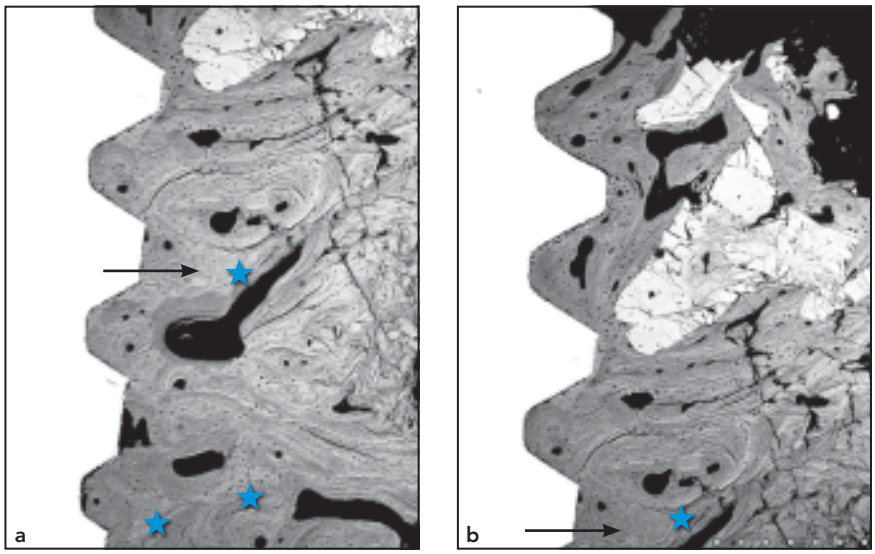

Fig 10a *Pre-existing interstitial bone is indicated by the blue stars on the SEM image. The darker-appearing bone apical to and surrounding the interstitial bone is actively remodeling pre-existing bone.*

Fig 10b *Three threads of new bone-to-implant contact are evident above the most coronal interstitial bone designated by the arrow and blue star. Remains of the bovine bone are visible away from the implant surface.*

dent, but particles of processing debris from the anodized surface are visible in the depression between the threads (Fig 9a). A higher-magnification SEM image shows the characteristic microanatomy of the pores of an additive anodized implant surface. The surface is free of bacteria, but some residual inorganic mineralized material is evident adjacent to and within the pores of the surface (Fig 9b).

The SEM images of the subcrestal implant core show pre-existing apical bone, remodeling pre-existing bone, new bone, and particles of bovine bone graft material. The pre-existing bone is denoted by the presence of interstitial bone, which stains lighter as it becomes more mineralized and has no rings (Fig 10a). The darker-appearing bone below and around the remnants of interstitial bone is actively remodeling old bone, and the ring structures are secondary osteons. Above the most coronal remnants of interstitial bone, in direct contact with the implant surface, is well-integrated new bone, evidenced by its relative lack of organization, increased cellularity, vascularity, number of marrow spaces, and incorporated particles of bovine graft material (Fig 10b).

The histology (Fig 11) expands on the findings of the subcrestal SEM photomicrographs. The section confirms the presence of dense new bone-to-implant contact against the top three threads coronal to the old bone with no evidence of epithelial or connective tissue downgrowth between the bone and the implant. There are no inflammatory cells visible against the implant or in the bone away from the implant surface. The particles of bovine bone that remain have moved away from the implant surface during the healing process to allow for direct apposition of new bone to the implant.

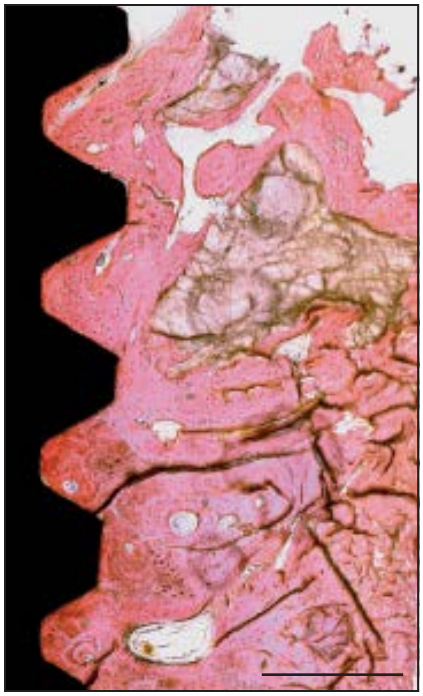

Fig 11 *The coronal three threads show direct osteocyte-to-implant contact with no epithelial or connective tissue cells intervening between the bone and the implant surface. The density of the new bone in the three threads approaches 100%. No inflammatory cells are evident near or away from the implant. The particles of residual graft material in the SEM image are also visible in this histologic section. Scale bar = 500 µm.*

Discussion

Reosseointegration, defined as histologic evidence of new direct bone-to-implant contact on a previously contaminated implant surface, has been demonstrated in experimentally created peri-implantitis defects in animals.[17–19] While human studies for the treatment of peri-implantitis have shown radiographic evidence of bone fill[20] and close bone-to-implant approximation on clinical reentry,[21,22] it is important to note these findings do not constitute evidence of reosseointegration. One human case of histologic reosseointegration using titanium granules as a graft material and ethylenediamenetetraacetic acid (EDTA) for surface decontamination has been published,[23] and the findings of this case report support and expand on the results of this research.

Low-cost, readily available instruments and medicaments were used in this study. While curettes are familiar to all dental professionals, their use for mechanical surface decontamination can be problematic. Metal curettes have been shown to alter the implant surface and damage the oxide layer, affecting surface chemistry and biocompatibility.[24] The tip of the curette should be softer than the implant material. While unfilled plastic resin curettes are one of the less effective means of removing plaque, they show the least amount of damage to a smooth implant surface[25] and can disrupt the biofilm colonies to facilitate their subsequent removal by chemical means.

The cost to chemically detoxify the implant surface with NaClO, H_2O_2, and SS was minimal. Small cotton pellets saturated with a solution were used to meticulously and firmly burnish the medicament onto the surface of the implant, especially between the threads. After the use of each antiseptic and at the completion of burnishing with SS, the entire peri-implant defect was irrigated thoroughly with SS. The purpose of this chemical decontamination was to kill the bacteria on the implant surface and remove the biofilm and the remaining bacterial cell wall endotoxin.

NaClO is a highly cytotoxic antiseptic and oxidizing agent that kills bacteria by denaturing its organic component. It is found naturally in macrophages and neutrophils, does not corrode titanium, and shows no visible effect on periodontal healing.[15] A solution of 0.25% NaClO, also known as Milton's solution, has been used for years for decontamination purposes and in periodontics for subgingival irrigation.[26]

H_2O_2 is also a widely available antiseptic. While it duplicates the oxidative effect of NaClO, in vitro research indicates it can remove cell wall lipopolysaccharide endotoxin[13] and enhance fibrinogen absorption, growth of the oxide layer, and deposition of calcium on the implant surface.[27] The implant surface appeared to be visually cleaner and brighter after its use.

SS has been shown in animal research to detoxify an implant surface to an extent that reosseointegration occurred.[17–19] In a human case history report following surface decontamination with SS, close bone-to-implant approximation was found on reentry.[21] Studies comparing detoxification agents have shown SS to be less effective than other medicaments, however.[14] Consequently, in this report NaClO and H_2O_2 were used in conjunction with SS for surface decontamination.

$CaSO_4$ and BB were used as bone-grafting materials. $CaSO_4$ is biocompatible, hemostatic, and anti-inflammatory; supports angiogenesis; and functions as a barrier membrane.[28] Its resorption stimulates osteoblastic activity as the calcium

ions released react with phosphate ions in the body, forming bone.[29] A human clinical case history report with a reentry showing close bone-to-implant approximation following grafting with calcium sulfate has been published.[21] BB has been shown to be a well-tolerated osteoconductive grafting agent[30] and was used as an adjunct in light of the large size of the osseous defect.

The porcine membrane used for guided bone regeneration was chosen for its handling characteristics. The punch technique allowed the membrane to be closely adapted 360 degrees around the implant, fully covering the bone graft (Fig 5b).

While heavy plaque and calculus accumulations were originally present on the implant threads (Fig 4a), the supracrestal surface was free of bacteria and relatively free of mineralized debris on reentry. Small particles of calcified material did remain within and around the micropores of the surface (Fig 9b). As a microbiologic assay was not performed it is not possible to determine whether the absence of soft tissue adherence was due to the calcified material remaining, residual endotoxin on the implant surface or within the screw access opening, or epithelial downgrowth due to the inherently weak nature of the connective tissue adherence to titanium.

In addition to initiating new bone formation, the decontamination procedure stimulated activity in the preexisting bone as areas of active osseous remodeling, identified by darker shading and the swirls of developing secondary osteons, are interspersed throughout the apical part of the photomicrograph (Fig 10a). Coronal to the remaining interstitial bone, an area of newly regenerated bone is present, evidenced by increased cellularity, vascularity, number of marrow spaces, and residual particles of grafted bovine bone. The top three threads show dense new direct bone-to-implant contact (Fig 10b).

The histologic section (Fig 11) expands to a cellular level the situation that is apparent in the SEMs. No inflammatory cells are evident either adjacent to or at a distance from the implant surface. Direct osteocyte-to-implant contact is present with no visible intervening epithelial or connective tissue cells. The bone-to-implant contact is dense, approaching 100%. It is unknown whether the $CaSO_4$ and bovine bone graft combination used in this patient, who initially had relatively dense bone, influenced the amount of reosseointegration.

There were eight exposed threads within the confines of the infrabony defect initially and five at the time of reentry. The three threads of new direct bone-to-implant contact in the photomicrographs confirm what was evident clinically and translate to a defect reintegration percentage of 37.5%. With an implant thread pitch of 0.6 mm, the height of new bone against the implant was calculated to be 1.8 mm. As human clinical reentries have been published showing what seem to be greater percentages of new bone-to-implant approximation in narrow infrabony defects,[20,21] it might be necessary to use a longer-lasting barrier and wait longer prior to reentry if higher percentages of reintegration are to be achieved in defects of this depth and width.

Conclusions

This case report supports and expands on the findings of previous animal and human histologic research. Reosseointegration, defined as histologic evidence of new direct bone-to-implant contact on a previously contaminated implant surface, is possible in a human. Equally significant is the finding that reosseointegration can occur following mechanical debridement and chemical surface decontamination using low-cost, readily available instruments and medicaments such as plastic curettes, dilute sodium hypochlorite, hydrogen peroxide, and sterile saline. Future research is needed to determine the technique's predictability on this implant surface and others.

Acknowledgments

The authors reported no conflicts of interest related to this study.

References

1. Albrektsson T, Buser D, Sennerby L. Crestal bone loss and oral implants. Clin Implant Dent Relat Res 2012;14:783–791.
2. Roos-Jansåker AM, Lindahl C, Renvert H, Renvert S. Nine- to fourteen-year follow-up of implant treatment. Part II: Presence of peri-implant lesions. J Clin Periodontol 2006;33:290–295.

3. Daubert D, Weinstein BF, Bordin S, Leroux BG, Flemming TF. Prevalence and predictive factors for peri-implant disease and implant failure: A cross-sectional analysis. J Periodontol 2015;86:337–347.
4. Derks J, Schaller D, Håkansson J, Wennström JL, Tomasi C, Berglundh T. Effectiveness of implant therapy analyzed in a Swedish population: Prevalence of peri-implantitis. J Dent Res 2016; 95:43–49.
5. Tomasi C, Derks J. Clinical research of peri-implant diseases—Quality of reporting, case definitions and methods to study incidence, prevalence and risk factors of peri-implant diseases. J Clin Periodontol 2012;39(suppl 12):207–223.
6. Atieh MA, Alsabeeha NH, Faggion CM Jr, Duncan WJ. The frequency of peri-implant diseases: A systematic review and meta-analysis. J Periodontol 2013;84: 1586–1598.
7. Zitzmann NU, Berglundh T. Definition and prevalence of peri-implant diseases. J Clin Periodontol 2008;35(suppl 8): 286–291.
8. Renvert S, Roos-Jansåker AM, Claffey N. Non-surgical treatment of peri-implant mucositis and peri-implantitis: A literature review. J Clin Periodontol 2008;35(suppl 8):305–315.
9. Ntrouka VF, Slot DE, Louropoulou A, Van der Weijden F. The effect of chemotherapeutic agents on contaminated titanium surfaces: A systematic review. Clin Oral Implants Res 2011;22:681–690.
10. Schmage P, Thielemann J, Nergiz I, Scorziello T, Pfeiffer P. Effects of 10 cleaning instruments on four different implant surfaces. Int J Oral Maxillofac Implants 2012;27:308–317.
11. Aoki A, Mizutani K, Schwarz F, et al. Periodontal and peri-implant wound healing following laser therapy. Periodontol 2000 2015;68:217–269.
12. Ramberg P, Lindhe J, Botticelli D, Botticelli A. The effect of a triclosan dentifrice on mucositis in subjects with dental implants: A six-month clinical study. J Clin Dent 2009;20:103–107.
13. Zablotsky MH, Diedrich DL, Meffert RM. Decontamination of endotoxin-contaminated titanium and hydroxyapatite-coated surfaces utilizing various chemotherapeutic and mechanical modalities. Implant Dent 1992;1:154–158.
14. Gosau M, Hahnel S, Schwarz F, Gerlach T, Reichert TE, Bürgers R. Effect of six different peri-implantitis disinfection methods on in vivo human oral biofilm. Clin Oral Implants Res 2010;21:866–872.
15. Slots J. Low-cost periodontal therapy. Periodontol 2000 2012;60:110–137.
16. Esposito M, Grusovin MG, Worthington HV. Treatment of peri-implantitis: What interventions are effective? A Cochrane systematic review. Eur J Oral Implantol 2012;5(suppl):S21–S41.
17. Persson L, Mouhyi J, Berglundh T, Sennerby L, Lindhe J. Carbon dioxide laser and hydrogen peroxide conditioning in the treatment of peri-implantitis: An experimental study in the dog. Clin Implant Dent Relat Res 2004;6:230–238.
18. Alhag M, Renvert S, Polyzois I, Claffey N. Re-osseointegration on rough implant surfaces previously coated with bacterial biofilm: An experimental study in the dog. Clin Oral Implants Res 2008; 4:182–187.
19. Kolonidis SG, Renvert S, Hammerle CH, Lang NP, Harris D, Claffey N. Osseointegration on implant surfaces previously contaminated with plaque. An experimental study in the dog. Clin Oral Implants Res 2003;14:373–380.
20. Schwarz F, Hegewald A, John G, Sahm N, Becker J. Four-year follow-up of combined surgical therapy of advanced peri-implantitis evaluating two methods of surface decontamination. J Clin Periodontol 2013;40:962–967.
21. Fletcher P, Constantinides C. Resolution of a peri-implantitis defect using sterile saline for implant surface detoxification: A case report with clinical re-entry. Clin Adv Periodontics 2015;5:235–241.
22. Froum SJ, Rosen P. Reentry evaluation following treatment of peri-implantitis with a regenerative approach. Int J Periodontics Restorative Dent 2014;34:47–59.
23. Wohlfahrt J, Aass AM, Ronold HJ, Lyngstadaas SP. Micro CT and human histological analysis of a peri-implant osseous defect grafted with porous titanium granules: A case report. Int J Oral Maxillofac Implants 2011;26:e9–e14.
24. Homiak AW, Cook PA, DeBoer J. Effect of hygiene instrumentation on titanium abutments: A scanning electron microscopy study. J Prosthet Dent 1992;67: 364–369.
25. Hasturk H, Nguyen DH, Sherzai H, et al. Comparison of the impact of scaler material composition on polished titanium implant abutment surfaces. J Dent Hyg 2013;87:200–211.
26. Galván M, Gonzalez S, Cohen C, et al. Periodontal effects of 0.25% sodium hypochlorite twice-weekly oral rinse. A pilot study. J Periodontol Res 2014;49:696–702.
27. Wälivaara B, Lundström I, Tengvall P. An in-vitro study of H_2O_2-treated titanium surfaces in contact with blood plasma and a simulated body fluid. Clin Mater 1993;12:141–148.
28. Mamidwar S, Arena C, Kelly S, Alexander H, Ricci J. In vitro characterization of a calcium sulfate/PLLA composite for use as a bone graft material. J Biomed Mater Res B Appl Biomater 2007;81:57–65.
29. Ricci J, Alexander H, Nadkarni P, et al. Biological mechanisms of calcium sulfate replacement by bone. In: Davies JE (ed). Bone Engineering. Toronto: EM Squared Inc, 2000.
30. Piattelli M, Favero G, Scarano A, Orsini G, Piattelli A. Bone reactions to anorganic bovine bone (Bio-oss) used in sinus augmentation procedures: Histologic long-term report of 20 cases in humans. Int J Oral Maxillofac Implants 1999;14: 835–840.